

---

# Implicit degree bias in the link prediction task

---

Rachith Aiyappa<sup>1</sup>, Xin Wang<sup>3</sup>, Munjung Kim<sup>1</sup>, Ozgur Can Seckin<sup>1</sup>,

Jisung Yoon<sup>2</sup>, Yong-Yeol Ahn<sup>1</sup>, Sadamori Kojaku<sup>3</sup>

<sup>1</sup>Center for Complex Networks and Systems Research, Luddy School of Informatics, Computing, and Engineering, Indiana University, Bloomington, IN, USA

<sup>2</sup>KDI School of Public Policy and Management, Sejong City, South Korea

<sup>3</sup>Department of Systems Science and Industrial Engineering, Binghamton University, Binghamton, NY, USA

{racball, munjkim, oseckin, yyahn}@iu.edu,  
jisung.yoon92@gmail.com, {xwang314, skojaku}@binghamton.edu

## Abstract

Link prediction—a task of distinguishing actual hidden edges from random unconnected node pairs—is one of the quintessential tasks in graph machine learning. Despite being widely accepted as a universal benchmark and a downstream task for representation learning, the validity of the link prediction benchmark itself has been rarely questioned. Here, we show that the common edge sampling procedure in the link prediction task has an implicit bias toward high-degree nodes and produces a highly skewed evaluation that favors methods overly dependent on node degree, to the extent that a “null” link prediction method based solely on node degree can yield nearly optimal performance. We propose a degree-corrected link prediction task that offers a more reasonable assessment that aligns better with the performance in the recommendation task. Finally, we demonstrate that the degree-corrected benchmark can more effectively train graph machine-learning models by reducing overfitting to node degrees and facilitating the learning of relevant structures in graphs.

## 1 Introduction

Standardized benchmarks such as ImageNet [1, 2] and SQuAD [3, 4] play a pivotal role in guiding the evolution of machine learning, creating a competitive environment that propels innovation by setting clear, measurable goals. A core benchmark for graph machine learning is the link prediction task, the task of identifying missing edges in a graph, with diverse applications including the recommendations of friends and contents [5–8], knowledge discoveries [9, 10], and drug development [11–17]. The link prediction benchmarks have been serving as a crucial benchmark that facilitates quantitative evaluations and drives the advancement of graph machine learning techniques [12, 16–21].

Despite its significant role in graph machine learning, the link prediction benchmark itself has rarely been examined critically for its effectiveness, reliability, and potential biases. A widely-used link prediction benchmark evaluates methods by their ability to classify pairs of nodes as either connected or unconnected [5, 18, 20]. The connected node pairs (i.e., edges) are randomly sampled from existing edges as the hidden positive set, and an equal number of node pairs are randomly chosen from unconnected node pairs. Existing criticisms mainly consider the disconnect from real-world scenarios.

For instance, unconnected node pairs are far more common than connected node pairs because of the sparsity of edges in graphs [22, 23], which can lead to biased performance evaluations [24–28]. Additionally, while the link prediction benchmark tests methods by classifying a predefined set of potential edges, the practical link prediction task involves identifying the potential edges from the entire graph. Despite the misalignment with real-world scenarios, high benchmark performance is often regarded as a testament to successful learning in graph machine learning [12, 15–18, 29–33].

Here, we argue that the standard link prediction benchmark has a fundamental and severe bias that favors methods that exploit node degree information (i.e., the number of edges a node has). The degree bias arises from the sampling of edges used for performance evaluations, i.e., when sampling an edge from a graph uniformly at random, a node with  $k$  edges is  $k$  times more likely to be selected than a node with a single edge ( $k = 1$ ). Meanwhile, the negative set of edges is randomly sampled from unconnected node pairs, which do not have this degree bias. As a result, we have a distinct and useful feature (degree) for the methods that can be leveraged without understanding any non-trivial structural features of the graph. We show that this degree bias is so profound that a “null” link prediction method based solely on node degree can yield nearly optimal performance, questioning the usefulness of the link prediction benchmark even as a general objective for graph machine learning and raising awareness on the need for being more intentional and careful about what the evaluation tasks themselves actually evaluate.

To address this bias, we propose a degree-corrected link prediction benchmark that samples the unconnected node pairs with the same degree bias. We demonstrate that the degree-corrected link prediction benchmark can better capture the performance of algorithms in the recommendation task. Moreover, we show that the degree-corrected benchmark trains graph neural networks more effectively by reducing overfitting to node degrees, thereby improving the learning of community structure in graphs.

## 2 Design flaw of the link prediction benchmark

**Preliminary** We focus on the unweighted, undirected graph  $G = (\mathcal{V}, \mathcal{E})$ , where  $\mathcal{V}$  is the set of nodes and  $\mathcal{E}$  is the set of edges. We assume that  $G$  has no self-loops, no multiple edges, and is highly sparse ( $|\mathcal{E}| \ll |\mathcal{V}|^2$ ), which is a common characteristic of real-world graphs [22, 23]. Degree  $k_i$  of a node  $i \in \mathcal{V}$  is the number of edges emanating from node  $i$ . We use  $\sim$  to denote proportional relationships. We exclude node attributes from data, if present, to ensure consistency across all graph-based link prediction methods.

**Link prediction benchmark** The standard procedure for link prediction benchmarks is outlined as follows [5, 12, 15–17, 29–33]. First, we randomly sample a fraction  $\beta$  of edges from the edge set  $\mathcal{E}$  as *positive edges*. Second, we randomly sample an equal number of unconnected node pairs with replacement from the node set  $\mathcal{V}$  as *negative edges*. We resample the negative edges if they form a loop or are already in the positive or test edges. Third, each node pair  $(i, j)$  is scored by a link prediction method, where a higher score  $s_{ij}$  indicates a higher likelihood of an edge existing between the nodes. Fourth, the effectiveness of a method is evaluated using the Area Under the Receiver Operating Characteristic Curve (AUC-ROC), which represents the probability that the method gives a higher score to a positive edge than a negative edge. While alternative benchmark designs use different evaluation metrics or sampling strategies for negative edges [24–28] (Section 4), this outlined procedure has been widely used [5, 12, 15–18, 29–32].

**Sampling bias due to node degree** A well-known, counterintuitive fact about graphs is that a uniform random sampling of edges results in a *biased* selection of nodes in terms of degree [34–38]. The bias arises because a node with  $k$  edges appears  $k$  times in the edge list and thus  $k$  times more likely to be chosen than a node with  $k' = 1$  edge (e.g., node 1 and 4 in Fig. 1A). Consequently, for a graph with degree distribution  $p(k)$ , the nodes in the positive edges have degree distribution  $p_{\text{pos}}(k)$  proportional to  $\sim k \cdot p(k)$ . By normalizing  $k \cdot p(k)$ , the degree distribution of the positive edges is given by

$$p_{\text{pos}}(k) = \frac{1}{\sum_{\ell} \ell p(\ell)} k \cdot p(k) = \frac{1}{\langle k \rangle} k \cdot p(k), \quad (1)$$

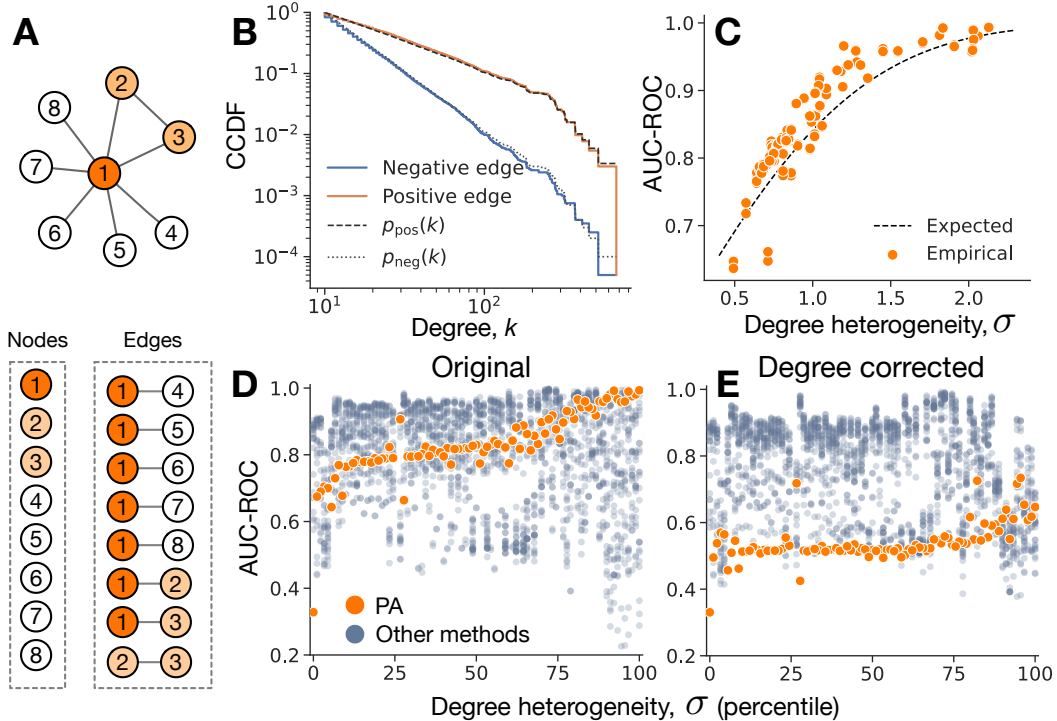


Figure 1: Illustration of the degree bias in the link prediction benchmark. **A**: A node with degree  $k$  appears  $k$  times in the edge list, making it  $k$  times more likely to be sampled as a positive edge than a node with degree 1. **B**: The degree distribution of the nodes in the positive and negative edges sampled from a Price graph of  $N = 10^5$  nodes and  $M = 10^6$  edges. The y-axis, “CCDF”, denotes the complementary cumulative distribution function, representing the probability that a node’s degree is at least  $k$ . Dashed lines illustrate the relationship described by Eq. (1). **C**: The AUC-ROC score for the Preferential Attachment (PA) method on empirical graphs, with the dashed line indicating the expected AUC-ROC based on the “null” link prediction method that uses only the node degree information (Eq. (9)). **D**: AUC-ROC of 26 methods across 90 graphs. PA outperforms 54% of the method on average across 90 graphs and outperforms most other methods in the most heterogeneous graphs. **E**: AUC-ROC of the same methods for the degree-corrected benchmark, showing that nearly 86% of the methods perform better than PA on average.

where  $\langle k \rangle$  is the average degree of the graph. On the other hand, the nodes in the negative edges are uniformly sampled from the node list (i.e.,  $\mathcal{V}$ ) and thereby have degree distribution  $p_{\text{neg}}(k)$  identical to  $p(k)$  (i.e.,  $p_{\text{neg}}(k) = p(k)$ ).

We demonstrate the degree bias using the Price graph of  $N = 10^5$  nodes and  $M = 10^6$  edges, with the power-law degree distribution approximating  $p(k) \propto k^{-3}$  (Fig. 1B). We sample  $\beta = 0.25$  of the edges uniformly at random from  $\mathcal{E}$  as positive edges, together with the same number of unconnected node pairs by uniformly sampling nodes from  $\mathcal{V}$ . The degree distributions for nodes in the positive and negative edges closely follow  $p_{\text{pos}}(k)$  and  $p_{\text{neg}}(k)$ , respectively, demonstrating the sampling bias due to node degree. We note that the degree bias is not specific to the Price graph but appears for any graph with non-uniform degree distribution.

**Impact of degree bias on the link prediction benchmark** We demonstrate the impact of degree bias on link prediction benchmark (Fig. 1D). We evaluated 26 link prediction methods across 90 graphs. These methods include 7 network topology-based methods (e.g., Common Neighbors (CN) [19]), 13 graph embedding methods (e.g., Laplacian EigenMap (EigenMap) [39]), 2 network models (e.g., Stochastic Block Model (e.g., SBM) [40]), and 4 graph neural networks (GNNs) (e.g., Graph Convolutional Network (GCN) [41]). Detailed descriptions of the methods and graphs are available in SI Section 1. We set the fraction of test edges to  $\beta = 0.25$  and repeat the experiment 5

times. We quantify the heterogeneity  $\sigma$  of node degree by fitting a log-normal distribution to  $p(k)$  and calculating its variance parameter  $\sigma$ . We will show that  $\sigma$  is a good indicator of the impact of degree bias in Section 2.

We focus on the Preferential Attachment (PA) link prediction method, which calculates the prediction score  $s_{ij} = k_i k_j$  using only node degrees. Although PA is a crude method that neglects key predictive features such as the number of common neighbors and shortest distance [24, 25, 29, 42, 43], it still outperforms more than half of the advanced methods with an average AUC-ROC of 0.83 (ranked 13th out of 26 methods; see Fig. 2A). PA performs better as the heterogeneity of node degrees increases. The outperformance of PA is attributed to the degree bias, where the positive edges are more likely to be formed by nodes with high degree and thereby are easily distinguishable from the negative edges. As a result, the current benchmark design favors methods that make predictions based largely on node degrees.

**Theoretical analysis** Many empirical graphs exhibit heterogeneous degree distributions, with a few nodes having an exceptionally large degree and most having a small degree. The heterogeneous degree distributions are often characterized by power-law degree distribution  $p(k) \propto k^{-\alpha}$  with  $\alpha \in (2, 3]$  (i.e., scale-free networks) [44–47] or log-normal distributions [48, 49]. While the power-law and log-normal distributions are both continuous, they are often used to characterize the discrete degree distribution and provide approximations [48–53]. We show that the AUC-ROC for PA reaches the nearly maximum under log-normal distributions with heterogeneous node degrees. See SI Section 2.2 for the case of power-law distributions.

Let us consider a general degree distribution  $p(k)$  without restricting ourselves to log-normal distributions. The AUC-ROC has a probabilistic interpretation [54]: it is the probability that the score  $s^+$  for the positive edges is larger than the score  $s^-$  for the negative edges. Recalling that PA computes  $s_{ij} = k_i k_j$ , the AUC-ROC for PA is given by

$$\text{AUC-ROC} = P(s_{i^-, j^-} \leq s_{i^+, j^+}) = P(k_{i^-} k_{j^-} \leq k_{i^+} k_{j^+}), \quad (2)$$

where  $i^\pm$  and  $j^\pm$  represent the nodes of the positive and negative edges, respectively. Now, let us assume that  $p(k)$  follows the log-normal distribution,  $\text{LogNorm}(k | \mu, \sigma^2)$ , given by [54]:

$$p(k) = \text{LogNorm}(k | \mu, \sigma^2) = \frac{1}{\sqrt{2\pi\sigma k}} \exp\left[-\frac{(\ln k - \mu)^2}{2\sigma^2}\right], \quad (3)$$

where  $\mu$  and  $\sigma$  are the parameters of the log-normal distribution. The mean of the log-normal degree distribution is  $\langle k \rangle = \exp(\mu + \sigma^2/2)$  [54]. By substituting Eq. (3) into Eq. (1), we derive the degree distribution of nodes in the positive edges as:

$$\begin{aligned} p_{\text{pos}}(k) &= \frac{k}{\langle k \rangle} \frac{1}{\sqrt{2\pi\sigma k}} \cdot \exp\left[-\frac{(\ln k - \mu)^2}{2\sigma^2}\right] \\ &= \frac{1}{\sqrt{2\pi\sigma k}} \exp\left[-\frac{1}{2\sigma^2} ((\ln k)^2 - 2\mu \ln k + \mu^2) + \ln k - \mu - \sigma^2/2\right] \\ &= \frac{1}{\sqrt{2\pi\sigma k}} \exp\left[-\frac{1}{2\sigma^2} ((\ln k)^2 - 2(\mu + \sigma^2) \ln k + \mu^2 + 2\mu\sigma^2 + \sigma^4)\right] \\ &= \frac{1}{\sqrt{2\pi\sigma k}} \exp\left[-\frac{(\ln k - \mu - \sigma^2)^2}{2\sigma^2}\right] = \text{LogNorm}(k | \mu + \sigma^2, \sigma^2). \end{aligned} \quad (4)$$

Equation (4) indicates that the degree distribution for nodes in the positive edges also follows a log-normal distribution, parameterized by  $\mu + \sigma^2$  and  $\sigma$ .

We derive the AUC-ROC for PA by leveraging a unique characteristic of log-normal distributions, i.e., the logarithm  $\ln k$  of log-normally-distributed degree  $k$  follows a normal distribution with mean  $\mu$  and variance  $\sigma^2$ , i.e.,

$$P(\ln k) = \text{Norm}(k | \mu, \sigma^2), \text{ where } \text{Norm}(k | \mu, \sigma^2) = \frac{1}{\sqrt{2\pi\sigma}} \exp\left[-\frac{(k - \mu)^2}{2\sigma^2}\right]. \quad (5)$$

We assume no degree assortativity in the graph, where  $P(k_i^+, k_j^+) = P(k_i)P(k_j)$ . Although empirical graphs often exhibit degree assortativity, our results indicate that it does not significantly impact the AUC-ROC (SI Section 2.1). For the negative edges, the distribution for  $\ln s_{i^-, j^-} =$

$\ln k_i^- + \ln k_j^-$  follows a normal distribution with mean  $2\mu$  and variance  $2\sigma^2$ , as the sum of independent normal variables also forms a normal distribution with additive means and variances [55], i.e.,

$$P(\ln s_{i-,j-}) = \text{Norm}(\ln s_{i-,j-} \mid 2\mu, 2\sigma^2). \quad (6)$$

For the positive edges, the degree distribution also follows a log-normal distribution (Eq. (4)). Thus, the distribution for  $\ln s_{i+,j+} = \ln k_i^+ + \ln k_j^+$  is given by

$$P(\ln s_{i+,j+}) = \text{Norm}(\ln s_{i+,j+} \mid 2\mu + 2\sigma^2, 2\sigma^2). \quad (7)$$

By using Eqs. (2), (6), and (7), we have

$$\begin{aligned} \text{AUC-ROC} &= P(\ln s^- < \ln s^+) \\ &= \int_{-\infty}^{\infty} \text{Norm}(x^- \mid 2\mu, 2\sigma^2) \left[ 1 - \int_{-\infty}^{x^-} \text{Norm}(x^+ \mid 2\mu + 2\sigma^2, 2\sigma^2) dx^+ \right] dx^- \\ &= 1 - \int_{-\infty}^{\infty} \text{Norm}(x^- \mid 2\mu, 2\sigma^2) \int_{-\infty}^{x^-} \text{Norm}(x^+ \mid 2\mu + 2\sigma^2, 2\sigma^2) dx^+ dx^- \end{aligned} \quad (8)$$

We reparameterize Eq. (8) by using  $z^\pm = \frac{x^\pm - 2\mu}{\sqrt{2}\sigma}$ . Noting that  $\text{Norm}(x^- \mid 2\mu, 2\sigma^2) \cdot \sqrt{2}\sigma = \text{Norm}(z^- \mid 0, 1)$  and  $dx^\pm = (\sqrt{2}\sigma)dz^\pm$ , we have

$$\begin{aligned} P(\ln s^- < \ln s^+) &= 1 - \int_{-\infty}^{\infty} (2\sigma^2) \text{Norm}(x^- \mid 2\mu, 2\sigma^2) \int_{-\infty}^{x^-} \text{Norm}(x^+ \mid 2\mu + 2\sigma^2, 2\sigma^2) \cdot dz^+ dz^- \\ &= 1 - \int_{-\infty}^{\infty} \text{Norm}(z^- \mid 0, 1) \int_{-\infty}^{z^-} \text{Norm}(z^+ - \sqrt{2}\sigma \mid 0, 1) dz^+ dz^- \\ &= 1 - \int_{-\infty}^{\infty} \text{Norm}(z^- \mid 0, 1) \Phi(z^- - \sqrt{2}\sigma) dz, \end{aligned} \quad (9)$$

where  $\Phi(z^-)$  is the cumulative distribution function for the standard normal distribution, i.e.,  $\Phi(z^-) = \int_{-\infty}^{z^-} \text{Norm}(y \mid 0, 1) dy$ . Equation (9) suggests the key behavior of AUC-ROC for PA. The AUC-ROC for PA is an increasing function of the parameter  $\sigma$  of the log-normal distribution (Fig. 1C). The parameter  $\sigma$  of the log-normal distribution controls the spread of the distribution, with larger  $\sigma$  resulting in a more fat-tailed distribution. While our assumptions about the log-normal degree distribution and degree assortativity may not always align with real-world data, Eq. (9) still effectively captures the AUC-ROC behavior for PA (Fig. 1C). Further analysis of power-law distributions is described in SI Section 2.2.

This theoretical result highlights the significant issue with the current link prediction benchmark: a high benchmark performance can be achieved by only learning node degrees, posing the question of whether the link prediction benchmark is an effective objective of graph machine learning.

### 3 The degree-corrected link prediction benchmark

The link prediction benchmark yields biased evaluations due to mismatched degree distributions between positive and negative edges, i.e.,  $p_{\text{neg}}(k) \neq p_{\text{pos}}(k)$ . To mitigate the mismatch, we introduce *the degree-corrected link prediction benchmark* that samples negative edges with the same degree bias as positive edges (Algorithm 1). Specifically, we create a list of nodes where each node with degree  $k$  appears  $k$  times. Then, we sample negative edges by uniformly sampling two nodes from this list with replacement until the sampled node pairs are not connected and not in the test edge set. Crucially, nodes with degree  $k$  are  $k$  times more likely to be sampled than nodes with degree 1, mirroring the degree bias of the positive edges. Consequently, the positive and negative edges in the degree-corrected benchmark are indistinguishable based on node degrees. A Python package for the degree-corrected benchmark is available at <https://github.com/skojaku/degree-corrected-link-prediction-benchmark>.

---

**Algorithm 1** Degree-corrected link prediction benchmark

---

- 1: **Input:** Graph  $G(\mathcal{V}, \mathcal{E})$ , Sampling fraction  $\beta \in [0, 1]$  for positive edges
  - 2: **Output:** Set of negative edges  $\mathcal{E}_{\text{neg}}$  and set of positive edges  $\mathcal{E}_{\text{pos}}$
  - 3: Generate  $\mathcal{E}_{\text{pos}}$  by randomly sampling  $\beta$  fraction of edges in  $\mathcal{E}$ .
  - 4: Initialize  $\mathcal{E}_{\text{neg}} \leftarrow \emptyset$
  - 5: Create a node list  $L$  where each node  $i \in \mathcal{V}$  with degree  $k_i$  appears  $k_i$  times
  - 6: **while**  $|\mathcal{E}_{\text{neg}}| < |\mathcal{E}_{\text{pos}}|$  **do**
  - 7:     Randomly select two nodes  $i, j$  from  $L$  with replacement
  - 8:     **if**  $(i, j) \notin \mathcal{E}$  and  $(i, j) \notin \mathcal{E}_{\text{neg}}$  and  $i \neq j$  **then**
  - 9:          $\mathcal{E}_{\text{neg}} \leftarrow \mathcal{E}_{\text{neg}} \cup \{(i, j)\}$
  - 10:     **end if**
  - 11: **end while**
  - 12: **return**  $\mathcal{E}_{\text{neg}}, \mathcal{E}_{\text{pos}}$
- 

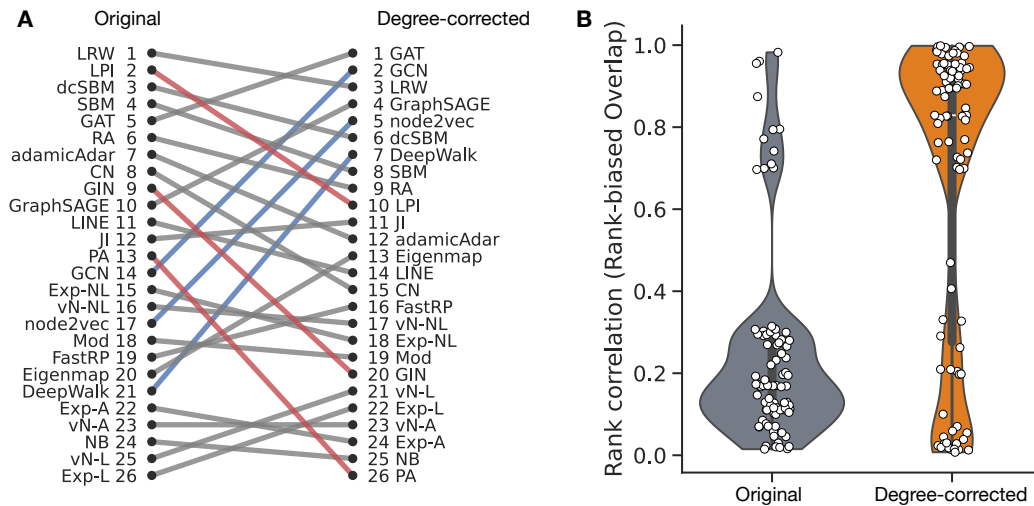


Figure 2: Comparative analysis of link prediction and recommendation benchmarks. **A:** Rank changes across the original and degree-corrected link prediction benchmarks. The red and blue lines indicate the methods that change their rankings more than 8 places from the original one. We compute the ranking of the methods based on the AUC-ROC of the link prediction benchmark and compare it against the ranking based on the link retrieval task. **B:** The degree-corrected benchmark ranks link prediction methods more similarly with the recommendation task than the original benchmark. The RBO (rank-biased overlap) represents the similarity between the ranking of the link prediction methods and that based on the recommendation task.

**Comparison of the benchmark evaluations** We reevaluated the methods with the degree-corrected link prediction benchmark (Fig. 1E). We use the same parameters in the original link prediction benchmark for all methods. There is some agreement between the original and degree-corrected benchmarks (Fig. 2A). For example, they rank GAT and LRW as top performers, while NB, SGTAdjNeu, and SGTAdjExp are consistently ranked lower. On the other hand, the degree-corrected benchmark ranks PA as the lowest performer, with its average AUC-ROC dropping from 0.83 to 0.54, placing it last out of 26 methods. The AUC-ROC near 0.5 for PA suggests that it performs as random guessing, confirming that the degree-corrected benchmark successfully makes the degree distributions of positive and negative edges indistinguishable. Other methods such as LPI, GIN also experience a substantial drop in their rankings from 2nd to 10th and 9th to 20th, respectively (Fig. 2A). On the other hand, GCN, node2vec, DeepWalk, and EigenMap increase their rankings substantially from 14th to 2nd, 17th to 5th, 21th to 7th, and 20th to 12th, respectively (Fig. 2A).

**The degree-corrected benchmark aligns better with recommendation tasks** Link prediction methods are often used in recommendation tasks [24–28]. However, there are key differences between

standard link prediction benchmarks and recommendation tasks [24–26]. In the link prediction benchmark, a set of potential edges is provided, and the goal is to determine the existence of these edges. In contrast, recommendation tasks require identifying potential edges from the entire graph without a preset list of candidate edges. This makes recommendation tasks more challenging due to the large number of unconnected nodes that could be just as likely to have an edge as connected nodes. For example, a link prediction task in a social network involves predicting friendships from a given list of potential friends. On the other hand, recommendation tasks must evaluate all potential unlisted friendships, including absent but equally probable friendships as existing ones. Nevertheless, given the common use of link prediction in recommendation tasks, it is crucial that the link prediction benchmarks accurately reflect the performance in the recommendation tasks.

We assess how well the link prediction benchmark provides coherent performance assessment with the recommendation task as follows. In the common recommendation task [25], the method recommends, for each node  $i$ , its top  $C = 50$  nodes  $j$  based on the highest scores  $s_{ij}$ . We note that our results are consistent regardless of the chosen  $C$  value (refer to SI Section 2.3). The effectiveness of the recommendations is then measured using the vertex-centric max precision recall at  $C$  (VCMPR@ $C$ ) defined as the higher of the precision and recall scores at  $C$  [25]. The VCMPR@ $C$  is designed to evaluate recommendation methods and addresses the excessive penalty on the precision scores at  $C$  for small-degree nodes, which often have low precision due to their limited number of edges. We perform this task five times and average the VCMPR@ $C$  scores across different runs.

For each graph, we evaluate the alignment between the rankings based on the recommendation task and those based on the link prediction benchmarks using Rank Biased Overlap (RBO) [56]. RBO is a ranking similarity metric with larger weights on the top performers in the two rankings. A larger RBO score indicates that the top performers in the two rankings are more similar. The weights on the top performer are controlled by the parameter  $p \in (0, 1)$ . While we set  $p = 0.5$  in our experiment, we confirmed that our results are robust to the choice of  $p$  (SI Section 2.3).

Our results from 90 graphs show that the degree-corrected benchmark achieves higher RBO scores than the original benchmark. We find consistent results for different values of  $C$  and parameter  $p$  of the RBO (SI Section 2.3). These results indicate that the degree-corrected benchmark more accurately mirrors the performance in recommendation tasks, providing a more reliable measure of the effectiveness of methods in practical applications.

**Degree-corrected benchmark facilitates the learning of community structure** The link prediction benchmark is a common unsupervised learning objective for GNNs [38, 57–59]. The degree bias implies that GNNs trained using the original link prediction benchmark tend to overfit to node degrees because they can easily differentiate between positive and negative edges based on node degrees. We show that the degree-corrected benchmark effectively prevents overfitting to node degrees and improves the learning of salient graph structures.

We evaluate GNNs on the common unsupervised task of community detection in graphs [40, 60, 61]. The community detection task identifies densely connected groups (i.e., communities) in a graph. Communities often correspond to functional units (e.g., social circles with similar opinions and protein complexes) in the graph, and detecting communities is a crucial task in many graph applications [40, 60–63]. Specifically, we test the GNNs by using the Lancichinetti-Fortunato-Radicchi (LFR) community detection benchmark [64], a standard benchmark for community detection [40, 61, 65, 66]. The LFR benchmark generates synthetic graphs with predefined communities as follows. Each node  $i$  is assigned a degree  $k_i$  from a power-law distribution  $p(k) \sim k^{-\tau_1}$ , with maximum degree  $k_{\max}$ . Nodes are randomly grouped into  $L$  communities, with community sizes (i.e., the number of nodes in a community) following another power-law distribution  $p(n) \sim n^{-\tau_2}$  bounded between  $n_{\min}$  and  $n_{\max}$ . Edges are then formed such that each node  $i$  connects to a fraction  $1 - \mu$  of its  $k_i$  edges within its community and the remaining fraction  $\mu$  to nodes in other communities. We generate 10 graphs for  $\mu \in \{0.05, 0.1, 0.15, \dots, 0.95, 1\}$  using the following parameter values: the number of nodes  $N = 3,000$ , the degree exponent  $\tau_1 \in \{2.5, 3\}$ , the average degree  $\langle k \rangle = 25$ , the maximum degree  $k_{\max} = 1000$ , the community-size exponent  $\tau_2 = 3$ , the minimum and maximum community size  $n_{\min} = 100$  and  $n_{\max} = 1000$ . We obtained qualitatively similar results for different values of the parameters of the LFR benchmark (SI Section 2.5).

We train GNNs using either the original or the degree-corrected link prediction benchmarks to minimize binary entropy loss in classifying the positive and negative edges. Using the trained GNNs, we generate node embeddings and apply the  $K$ -means clustering algorithm to detect communities,

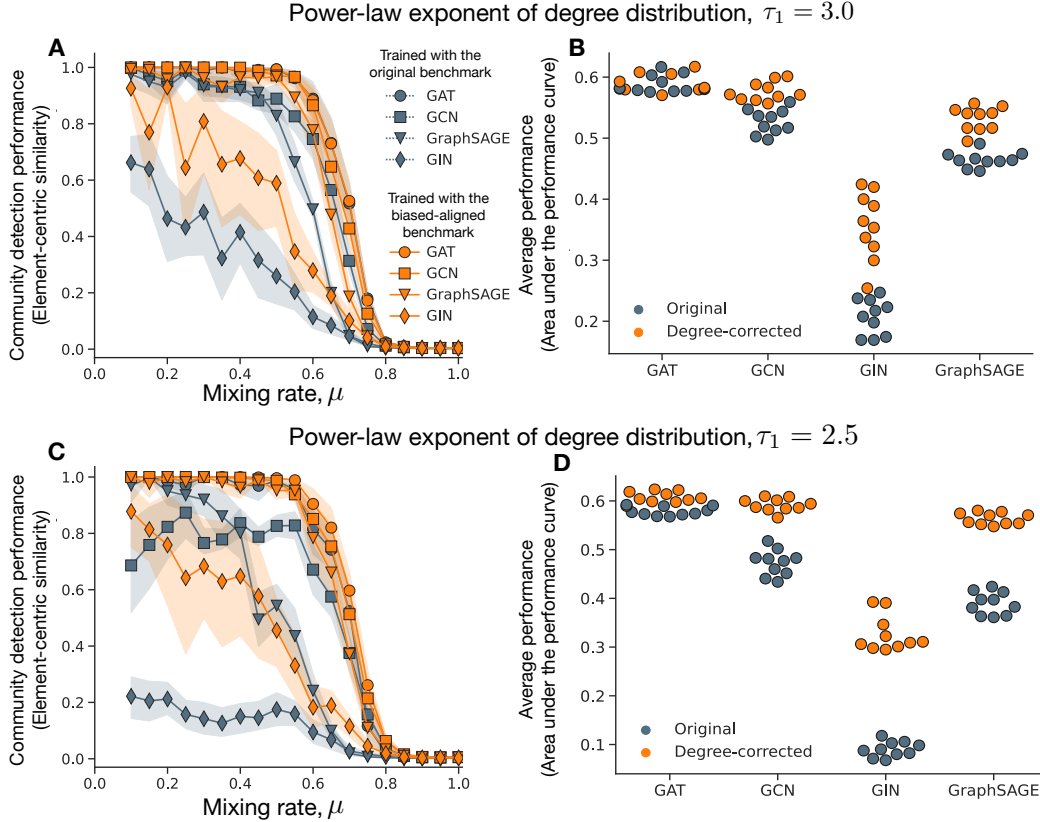


Figure 3: The degree-corrected benchmark improves GNNs in learning community structure in the LFR graphs. The LFR graphs consist of 3,000 nodes with the average degree of 25. **A**: The performance of community detection for the LFR graphs with a power-law degree distribution with  $\tau_1 = 3.0$  as a function of  $\mu$ . **B**: The average performance (by the area under the performance curve) shows that the methods trained with the degree-corrected training set outperform their counterparts trained with the traditional link prediction training set. **C**, **D**: The same plots for LFR graphs with a fatter power-law degree distribution with  $\tau_1 = 2.5$ . The error bars represent the 95% confidence interval estimated by a bootstrap of 1,000 repetitions.

where  $K$  is set to the number of true communities. Although the number  $K$  of communities is often unknown, we use the ground-truth number to eliminate noise from estimating  $K$  and to concentrate on evaluating the quality of the learned node embeddings, a standard practice in benchmarking node embeddings for the community detection task [65–67]. We measure the performance of GNNs by comparing the detected communities against the true communities using the adjusted element-centric similarity [66–68], where higher scores indicate a higher similarity between the node partitions for the true and detected communities. We observe qualitatively similar results for partition similarities based on the normalized mutual information (SI Section 2.4).

All GNNs, except for GIN, perform well when  $\mu \leq 0.5$ , where communities are distinct and easily identifiable, but their performance declines as  $\mu$  increases (Fig. 3A). Across a broad range of  $\mu$ , degree-corrected GNNs, particularly GIN, GCN, and GraphSAGE, outperform original GNNs in identifying communities, as shown by the area under the performance curve (Fig. 3B). The advantage of degree-corrected benchmarks becomes more evident with a more heterogeneous degree distribution (Fig. 3C and D). This indicates that degree correction effectively reduces overfitting to node degrees, enhancing the learning of community structures in graphs.

## 4 Discussion

We showed that the common link prediction benchmark suffered from a sampling bias arising from node degree and could mislead performance evaluations by favoring methods that overfit to node degree. To address this issue, we proposed a degree-corrected benchmark that corrected the discrepancy between the degree distributions of the connected and unconnected node pairs sampled for performance evaluation. This new benchmark provided more accurate evaluations that aligned better with the performance for recommendation tasks and also improved training for GNNs by reducing the overfitting to node degree and facilitating the learning of communities in the graph.

While we focused on node degree, other features can also effectively distinguish between positive and negative edges [24, 29, 42, 43]. Previous studies showed that nodes in the negative edge set tend to be distant from each other, making them easily identifiable by computing the distance between nodes [24, 42]. Our findings add a new direction to the important examination of the fundamental graph machine-learning task by demonstrating that node degree, a simpler structural attribute, is sufficient, in many cases, for differentiating the positive and negative edges. We note that the degree bias partially accounts for the distance discrepancy in the positive and negative edges because a high degree heterogeneity can induce loops of short length in the graph [69]. Crucially, the degree bias stems from the degree distribution rather than the connections between nodes and thus is present in any non-regular graph. More broadly, the degree bias is manifested through the edge sampling process, a general technique for evaluating and training graph machine learning. For instance, mini-batch training [57, 70], which samples subsets of edges for efficient GNN training, may also exhibit bias due to node degrees, leading to skewed training sets. Given the widespread use of edge sampling across various graph machine-learning tasks, our findings have broad implications beyond link prediction benchmarks, extending to a range of benchmarks and training frameworks.

Our study has several limitations. First, we employed standard hyperparameters (e.g., embedding dimensions, GNN layers) across all link prediction methods, achieving reasonable performance in link prediction and community detection tasks. Given the extensive variety of methods and hyperparameters, we did not optimize hyperparameters for specific tasks. Although fine-tuning could potentially enhance performance [24], our primary goal was to evaluate the effectiveness of link prediction benchmarks, not to compare the difference in performances between different link prediction methods. Second, we did not explore the reasons behind the varying performance of different link prediction methods. It is important to note that there is no single link prediction method that is universally effective for all graphs because the performance of link prediction methods depends on the assumptions on the graph structure to make the predictions [18]. Future studies will explore an in-depth examination of the link prediction methods on specific graphs. Third, we focus on community structure to test the effectiveness of the proposed benchmark as a training framework. However, other non-trivial graph structures, such as centrality, could be tested through network dismantling benchmarks [71].

Even with the aforementioned limitations, our results suggest that sampling graph data is a highly non-trivial task than commonly considered. Because sampling edges from a graph is integral to evaluating and training graph machine learning methods, our results underline the importance of careful sampling to ensure the effectiveness of evaluations and training of graph machine learning methods.

## 5 Broader Impacts

Our findings indicate that the standard benchmark promotes link prediction algorithms that enhance the “rich-get-richer” effect, where well-connected nodes tend to gain even more connections. This effect, known as *preferential attachment*, is common in various societal contexts. For instance, popular individuals often gain more friends, widely shared content spreads further, and frequently cited papers are more likely to attract additional citations. While preferential attachment can benefit distributing resources and recognition, it also presents significant disadvantages. For example, preferential attachment can disproportionately favor well-connected individuals in professional networks and hinder scientific progress by undervaluing innovative papers with less citations [72]. Our analysis indicates that the recommendation algorithms trained using the existing benchmark may exacerbate social inequalities by reinforcing the preferential attachment mechanism. Our new benchmark directly

addresses these concerns by negating the degree bias, promoting fairer algorithm evaluations, and supporting the development of fairness-aware machine learning methods.

**Code and Data Availability** We provide the code to reproduce the results in this study at <https://github.com/skojaku/degree-corrected-link-prediction-benchmark>. The network data used in this study is available at [https://figshare.com/projects/Implicit\\_degree\\_bias\\_in\\_the\\_link\\_prediction\\_task/205432](https://figshare.com/projects/Implicit_degree_bias_in_the_link_prediction_task/205432).

## Acknowledgments and Disclosure of Funding

R.A., M.K., O.C.S., S.K., and Y.Y.A. acknowledge the support by the Air Force Office of Scientific Research under award number FA9550-19-1-0391. The authors acknowledge the computing resources at Binghamton University and Indiana University and thank NVIDIA Corporation for their GPU resources.

## References

- [1] Jia Deng, Wei Dong, Richard Socher, Li-Jia Li, Kai Li, and Li Fei-Fei. Imagenet: A large-scale hierarchical image database. In *2009 IEEE conference on computer vision and pattern recognition*, pages 248–255. IEEE, 2009.
- [2] Alex Krizhevsky, Ilya Sutskever, and Geoffrey E Hinton. Imagenet classification with deep convolutional neural networks. *Advances in Neural Information Processing Systems*, 25, 2012.
- [3] Pranav Rajpurkar, Jian Zhang, Konstantin Lopyrev, and Percy Liang. SQuAD: 100,000+ questions for machine comprehension of text. In Jian Su, Kevin Duh, and Xavier Carreras, editors, *Proceedings of the 2016 Conference on Empirical Methods in Natural Language Processing*, pages 2383–2392, Austin, Texas, November 2016. Association for Computational Linguistics.
- [4] Pranav Rajpurkar, Robin Jia, and Percy Liang. Know what you don’t know: Unanswerable questions for SQuAD. In Iryna Gurevych and Yusuke Miyao, editors, *Proceedings of the 56th Annual Meeting of the Association for Computational Linguistics (Volume 2: Short Papers)*, pages 784–789, Melbourne, Australia, July 2018. Association for Computational Linguistics.
- [5] Jérôme Kunegis and Andreas Lommatzsch. Learning spectral graph transformations for link prediction. In *Proceedings of the 26th Annual International Conference on Machine Learning*, pages 561–568, 2009.
- [6] Peng Wang, Baowen Xu, Yurong Wu, and Xiaoyu Zhou. Link prediction in social networks: the state-of-the-art. *Science China Information Sciences*, pages 1–38, 2014.
- [7] Zan Huang, Xin Li, and Hsinchun Chen. Link prediction approach to collaborative filtering. In *Proceedings of the 5th ACM/IEEE-CS joint conference on Digital libraries*, pages 141–142, 2005.
- [8] Aditya Krishna Menon and Charles Elkan. Link prediction via matrix factorization. In *Machine Learning and Knowledge Discovery in Databases: European Conference, ECML PKDD 2011, Athens, Greece, September 5-9, 2011, Proceedings, Part II 22*, pages 437–452. Springer, 2011.
- [9] Zhiqing Sun, Zhi-Hong Deng, Jian-Yun Nie, and Jian Tang. Rotate: Knowledge graph embedding by relational rotation in complex space. In *International Conference on Learning Representations*, 2019.
- [10] Antoine Bordes, Nicolas Usunier, Alberto Garcia-Duran, Jason Weston, and Oksana Yakhnenko. Translating embeddings for modeling multi-relational data. *Advances in Neural Information Processing Systems*, 26, 2013.
- [11] Khushnood Abbas, Alireza Abbasi, Shi Dong, Ling Niu, Laihang Yu, Bolun Chen, Shi-Min Cai, and Qambar Hasan. Application of network link prediction in drug discovery. *BMC Bioinformatics*, 22:1–21, 2021.
- [12] Anna Breit, Simon Ott, Asan Agibetov, and Matthias Samwald. Openbiolink: a benchmarking framework for large-scale biomedical link prediction. *Bioinformatics*, 36(13):4097–4098, 2020.
- [13] Jiaying You, Robert D McLeod, and Pingzhao Hu. Predicting drug-target interaction network using deep learning model. *Computational biology and chemistry*, 80:90–101, 2019.
- [14] Sheng-Min Wang, Hae-Kook Lee, Yong-Sil Kweon, Chung Tai Lee, and Kyoung-Uk Lee. Overactive bladder successfully treated with duloxetine in a female adolescent. *Clinical Psychopharmacology and Neuroscience*, 13(2):212, 2015.
- [15] Gamal Crichton, Yufan Guo, Sampo Pyysalo, and Anna Korhonen. Neural networks for link prediction in realistic biomedical graphs: a multi-dimensional evaluation of graph embedding-based approaches. *BMC Bioinformatics*, 19:1–11, 2018.

- [16] Xiang Yue, Zhen Wang, Jingong Huang, Srinivasan Parthasarathy, Soheil Moosavinasab, Yungui Huang, Simon M Lin, Wen Zhang, Ping Zhang, and Huan Sun. Graph embedding on biomedical networks: methods, applications and evaluations. *Bioinformatics*, 36(4):1241–1251, 2020.
- [17] Mehdi Ali, Charles Tapley Hoyt, Daniel Domingo-Fernández, Jens Lehmann, and Hajira Jabeen. Biokeen: a library for learning and evaluating biological knowledge graph embeddings. *Bioinformatics*, 35(18):3538–3540, 2019.
- [18] Amir Ghasemian, Homa Hosseinmardi, Aram Galstyan, Edoardo M Airoidi, and Aaron Clauset. Stacking models for nearly optimal link prediction in complex networks. *Proceedings of the National Academy of Sciences*, 117(38):23393–23400, 2020.
- [19] David Liben-Nowell and Jon Kleinberg. The link prediction problem for social networks. In *Proceedings of the Twelfth International Conference on Information and Knowledge Management, CIKM '03*, page 556–559, New York, NY, USA, 2003. Association for Computing Machinery.
- [20] Alexandru Cristian Mara, Jeffrey Lijffijt, and Tijn De Bie. Benchmarking network embedding models for link prediction: Are we making progress? In *2020 IEEE 7th International conference on data science and advanced analytics (DSAA)*, pages 138–147. IEEE, 2020.
- [21] Arvind Narayanan, Elaine Shi, and Benjamin IP Rubinfeld. Link prediction by de-anonymization: How we won the kaggle social network challenge. In *The 2011 International Joint Conference on Neural Networks*, pages 1825–1834. IEEE, 2011.
- [22] Mark EJ Newman. Network structure from rich but noisy data. *Nature Physics*, 14(6):542–545, 2018.
- [23] Albert-László Barabási and Márton Pósfai. *Network Science*. Cambridge University Press, Cambridge, United Kingdom, 1st edition edition, 2016.
- [24] Juanhui Li, Harry Shomer, Haitao Mao, Shenglai Zeng, Yao Ma, Neil Shah, Jiliang Tang, and Dawei Yin. Evaluating graph neural networks for link prediction: Current pitfalls and new benchmarking. *Advances in Neural Information Processing Systems*, 36, 2024.
- [25] Nicolas Menand and C Seshadhri. Link prediction using low-dimensional node embeddings: The measurement problem. *Proceedings of the National Academy of Sciences*, 121(8):e2312527121, 2024.
- [26] Yang Yang, Ryan N Lichtenwalter, and Nitesh V Chawla. Evaluating link prediction methods. *Knowledge and Information Systems*, 45:751–782, 2015.
- [27] Zexi Huang, Mert Kosan, Arlei Silva, and Ambuj Singh. Link prediction without graph neural networks. *arXiv preprint arXiv:2305.13656*, 2023.
- [28] Zhitao Wang, Yong Zhou, Litao Hong, Yuanhang Zou, Hanjing Su, and Shouzhi Chen. Pairwise learning for neural link prediction. *arXiv preprint arXiv:2112.02936*, 2021.
- [29] Muhan Zhang and Yixin Chen. Link prediction based on graph neural networks. *Advances in Neural Information Processing Systems*, 31, 2018.
- [30] Aditya Grover and Jure Leskovec. Node2vec: Scalable Feature Learning for Networks. In *Proceedings of the 22nd ACM SIGKDD International Conference on KDD, KDD '16*, pages 855–864, New York, NY, USA, 2016. Association for Computing Machinery.
- [31] Mingdong Ou, Peng Cui, Jian Pei, Ziwei Zhang, and Wenwu Zhu. Asymmetric transitivity preserving graph embedding. In *Proceedings of the 22nd ACM SIGKDD International Conference on Knowledge discovery and data mining*, pages 1105–1114, 2016.
- [32] Palash Goyal and Emilio Ferrara. Graph embedding techniques, applications, and performance: A survey. *Knowledge-Based Systems*, 151:78–94, 2018.
- [33] Lei Cai, Jundong Li, Jie Wang, and Shuiwang Ji. Line graph neural networks for link prediction. *IEEE Transactions on Pattern Analysis and Machine Intelligence*, 44(9):5103–5113, 2021.
- [34] Scott L Feld. Why your friends have more friends than you do. *American journal of sociology*, 96(6):1464–1477, 1991.
- [35] Marc Barthélemy, Alain Barrat, Romualdo Pastor-Satorras, and Alessandro Vespignani. Velocity and hierarchical spread of epidemic outbreaks in scale-free networks. *Physical Review letters*, 92(17):178701, 2004.
- [36] Nicholas A Christakis and James H Fowler. Social network sensors for early detection of contagious outbreaks. *PLoS ONE*, 5(9):e12948, 2010.
- [37] Sadamori Kojaku, Laurent Hébert-Dufresne, Enys Mones, Sune Lehmann, and Yong-Yeol Ahn. The effectiveness of backward contact tracing in networks. *Nature Physics*, 17(5):652–658, 2021.
- [38] Sadamori Kojaku, Jisung Yoon, Isabel Constantino, and Yong-Yeol Ahn. Residual2vec: Debiasing graph embedding with random graphs. *Advances in Neural Information Processing Systems*, 34:24150–24163, 2021.

- [39] Mikhail Belkin and Partha Niyogi. Laplacian Eigenmaps for Dimensionality Reduction and Data Representation. *Neural Computation*, 15(6):1373–1396, 2003.
- [40] Santo Fortunato. Community detection in graphs. *Physics Reports*, 486(3):75–174, 2010.
- [41] Thomas N. Kipf and Max Welling. Semi-supervised classification with graph convolutional networks. In *International Conference on Learning Representations (ICLR)*, 2017.
- [42] Ryan Lichtnwalter and Nitesh V Chawla. Link prediction: fair and effective evaluation. In *2012 IEEE/ACM International Conference on Advances in Social Networks Analysis and Mining*, pages 376–383. IEEE, 2012.
- [43] Haitao Mao, Juanhui Li, Harry Shomer, Bingheng Li, Wenqi Fan, Yao Ma, Tong Zhao, Neil Shah, and Jiliang Tang. Revisiting link prediction: A data perspective. *arXiv preprint arXiv:2310.00793*, 2023.
- [44] Réka Albert and Albert-László Barabási. Statistical mechanics of complex networks. *Reviews of modern physics*, 74(1):47, 2002.
- [45] Albert-László Barabási and Eric Bonabeau. Scale-free networks. *Scientific american*, 288(5):60–69, 2003.
- [46] Petter Holme. Rare and everywhere: Perspectives on scale-free networks. *Nature communications*, 10(1):1016, 2019.
- [47] Ivan Voitalov, Pim Van Der Hoorn, Remco Van Der Hofstad, and Dmitri Krioukov. Scale-free networks well done. *Physical Review Research*, 1(3):033034, 2019.
- [48] Igor Artico, I Smolyarenko, Veronica Vinciotti, and Ernst C Wit. How rare are power-law networks really? *Proceedings of the Royal Society A*, 476(2241):20190742, 2020.
- [49] Anna D Broido and Aaron Clauset. Scale-free networks are rare. *Nature communications*, 10(1):1017, 2019.
- [50] Aaron Clauset, Cosma Rohilla Shalizi, and Mark EJ Newman. Power-law distributions in empirical data. *SIAM review*, 51(4):661–703, 2009.
- [51] Filippo Radicchi, Santo Fortunato, and Claudio Castellano. Universality of citation distributions: Toward an objective measure of scientific impact. *Proceedings of the National Academy of Sciences*, 105(45):17268–17272, 2008.
- [52] Norman L Johnson, Samuel Kotz, and Narayanaswamy Balakrishnan. *Continuous univariate distributions, volume 2*, volume 289. John wiley & sons, 1995.
- [53] Sidney Redner. Citation statistics from 110 years of physical review. *Physics today*, 58(6):49–54, 2005.
- [54] David J Hand. Measuring classifier performance: a coherent alternative to the area under the roc curve. *Machine learning*, 77(1):103–123, 2009.
- [55] Christopher M Bishop. Pattern recognition and machine learning. *Springer google schola*, 2:1122–1128, 2006.
- [56] William Webber, Alistair Moffat, and Justin Zobel. A similarity measure for indefinite rankings. *ACM Trans. Inf. Syst.*, 28(4), nov 2010.
- [57] Will Hamilton, Zhitao Ying, and Jure Leskovec. Inductive representation learning on large graphs. *Advances in Neural Information Processing Systems*, 30, 2017.
- [58] Tatsuhiro Kawamoto, Masashi Tsubaki, and Tomoyuki Obuchi. Mean-field theory of graph neural networks in graph partitioning. *Advances in Neural Information Processing Systems*, 31, 2018.
- [59] Jian Tang, Meng Qu, Mingzhe Wang, Ming Zhang, Jun Yan, and Qiaozhu Mei. LINE: Large-scale Information Network Embedding. In *Proceedings of the 24th International Conference on World Wide Web, WWW '15*, pages 1067–1077, Republic and Canton of Geneva, CHE, 2015. International World Wide Web Conferences Steering Committee.
- [60] Santo Fortunato and Mark E. J. Newman. 20 years of network community detection. *Nature Physics*, 18(8):848–850, 2022.
- [61] Santo Fortunato and Darko Hric. Community detection in networks: A user guide. *Physics Reports*, 659:1–44, 2016.
- [62] Tiago P. Peixoto. Parsimonious module inference in large networks. *Physical Review Letters*, 110(14):148701, 2013.
- [63] Tiago P Peixoto. Reconstructing networks with unknown and heterogeneous errors. *Physical Review X*, 8(4):041011, 2018.
- [64] Andrea Lancichinetti, Santo Fortunato, and Filippo Radicchi. Benchmark graphs for testing community detection algorithms. *Physical Review E*, 78(4):046110, 2008.

- [65] Aditya Tandon, Aiiad Albeshri, Vijey Thayananthan, Wade Alhalabi, Filippo Radicchi, and Santo Fortunato. Community detection in networks using graph embeddings. *Physical Review E*, 103(2):022316, 2021.
- [66] Sadamori Kojaku, Filippo Radicchi, Yong-Yeol Ahn, and Santo Fortunato. Network community detection via neural embeddings. *arXiv preprint arXiv:2306.13400*, 2023.
- [67] Bianka Kovács, Sadamori Kojaku, Gergely Palla, and Santo Fortunato. Iterative embedding and reweighting of complex networks reveals community structure. *arXiv preprint arXiv:2402.10813*, 2024.
- [68] Alexander J. Gates, Ian B. Wood, William P. Hetrick, and Yong-Yeol Ahn. Element-centric clustering comparison unifies overlaps and hierarchy. *Scientific Reports*, 9(1):8574, 2019.
- [69] Ginestra Bianconi and Matteo Marsili. Loops of any size and hamilton cycles in random scale-free networks. *Journal of Statistical Mechanics: Theory and Experiment*, 2005(06):P06005, 2005.
- [70] Ziniu Hu, Yuxiao Dong, Kuansan Wang, and Yizhou Sun. Heterogeneous graph transformer. In *Proceedings of the Web Conference 2020*, pages 2704–2710, 2020.
- [71] Saeed Osat, Fragkiskos Papadopoulos, Andreia Sofia Teixeira, and Filippo Radicchi. Embedding-aided network dismantling. *Physical Review Research*, 5(1):013076, 2023.
- [72] Johan SG Chu and James A Evans. Slowed canonical progress in large fields of science. *Proceedings of the National Academy of Sciences*, 118(41):e2021636118, 2021.

# Supplementary Information for “Implicit degree bias in the link prediction task”

## Contents

<b>1</b>	<b>Data and link prediction methods</b>	<b>2</b>
1.1	Network data . . . . .	2
1.2	Link prediction algorithms . . . . .	2
1.2.1	Topology-based predictors . . . . .	2
1.2.2	Graph embeddings . . . . .	2
1.2.3	Graph Neural Networks . . . . .	3
1.2.4	Network models . . . . .	4
1.3	Additional analysis methods . . . . .	4
<b>2</b>	<b>Robustness analysis</b>	<b>5</b>
2.1	Impact of degree assortativity on the AUC-ROC for PA . . . . .	5
2.2	AUC-ROC for PA for scale-free networks . . . . .	6
2.3	Parameter sensitivity in the analysis of performance alignment with the recommendation task . . . . .	8
2.4	Evaluation of the community detection performance using the normalized mutual information . . . . .	8
2.5	Sensitivity to the choice of the LFR benchmark parameters . . . . .	9
<b>3</b>	<b>Reproducibility</b>	<b>9</b>
3.0.1	Source data and code . . . . .	9
3.0.2	Snakemake workflow . . . . .	9
3.0.3	Execution time and hardware requirements . . . . .	10

# 1 Data and link prediction methods

## 1.1 Network data

The corpus of networks used in this work comprises networks with the number of nodes in the range  $[10^2, 10^6]$  and edges in the range  $[10^2, 10^8]$ . This includes social, technological, information, biological, and transportation (spatial) networks. For simplicity in our analysis, we consider these networks to be unweighted, undirected, and without self-loops, though the message of our work holds without these constraints. The largest networks in our corpus (number of nodes  $> 10^5$ ) are sourced from Netzschleuder [1], and the remaining networks are obtained from the authors of Ref. [2]. See Table 2 for details.

## 1.2 Link prediction algorithms

We use 26 link prediction algorithms categorized into four groups: topology-based, graph embedding, network model, and graph neural networks (see Table 1).

### 1.2.1 Topology-based predictors

Topology-based predictors calculate the prediction score  $s_{ij}$  using the structural features of two nodes. The topology-based predictors employed in our study include Preferential Attachment (PA) [3], Common Neighbors (CN) [4], Adamic-Adar (AA) [5], Jaccard Index (JI) [4], Resource Allocation (RA) [6, 7], Local Random Walk (LRW) [8], Local Path Index (LPI) [9]. For LRW and LPI, we set the hyperparameter  $\epsilon = 0.001$  as per previous studies [8, 9]. The other methods do not require hyperparameters.

### 1.2.2 Graph embeddings

Graph embedding maps a graph into a vector space, with each node  $i$  represented by a point in this space. The prediction score  $s_{ij}$  is given by the dot product  $\mathbf{u}_i^\top \mathbf{u}_j$  between any two node vectors. We tested a variety of graph embedding methods including Laplacian EigenMap (EigenMap) [10], Spectral Modularity (Mod) [11], Non-backtracking Embedding (NB) [12], FastRP (FastRP) [13], Exponential Kernel on Adjacency Matrix (Exp-A) [14, 15], Exponential Kernel on Laplacian (Exp-L) [14, 15], Exponential Kernel on

Normalized Laplacian (Exp-NL) [14, 15], Von Neumann Kernel on Adjacency Matrix (vN-A) [15, 16], Von Neumann Kernel on Laplacian (vN-L) [15, 16], and Von Neumann Kernel on Normalized Laplacian (vN-NL) [15, 16], node2vec (node2vec) [17], DeepWalk (DeepWalk) [18], and LINE (LINE) [19]. We tested a variety of graph embedding methods including Laplacian EigenMap (EigenMap) [10], Spectral Modularity (Mod) [11], Non-backtracking Embedding (NB) [12], FastRP (FastRP) [13], Exponential Kernel on Adjacency Matrix (Exp-A) [14, 15], Exponential Kernel on Laplacian (Exp-L) [14, 15], Exponential Kernel on Normalized Laplacian (Exp-NL) [14, 15], Von Neumann Kernel on Adjacency Matrix (vN-A) [15, 16], Von Neumann Kernel on Laplacian (vN-L) [15, 16], and Von Neumann Kernel on Normalized Laplacian (vN-NL) [15, 16], node2vec (node2vec) [17], DeepWalk (DeepWalk) [18], and LINE (LINE) [19]. For all methods, we set the number of embedding dimensions to 128. For LINE, node2vec, and DeepWalk, we set the number of walkers to 40 and the number of the walk length to 80 following Ref. [20]. We used the default hyperparameters used in the original papers unless otherwise specified.

### 1.2.3 Graph Neural Networks

Graph neural networks (GNNs) learn the vector representation,  $\mathbf{u}_i$ , for each node  $i$  of the network by using neural networks. The prediction score  $s_{ij}$  is given by the dot product  $\mathbf{u}_i^\top \mathbf{u}_j$  between any two node vectors. We also explore several graph neural network (GNN) architectures for link prediction, leveraging the PyTorch Geometric library [21]. The GNN methods we employ include: Graph Convolutional Network (GCN) [22], Graph SAGE (GraphSAGE) [23], Graph Attention Network (GAT) [24], and Graph Isomorphism Network (GIN) [25]. We use two hidden layers of 256 dimensions with ReLU activation and a linear output layer of 128 dimensions. The node features are the 64 principal eigenvectors of the adjacency matrix, and we extend the feature vector by adding a 64-dimensional vector with each element being generated from an independent Gaussian distribution with mean 0 and standard deviation 1 by following Ref. [26, 27]. We train GNNs on the link prediction task for 250 epochs with a dropout rate of 0.2, using the Adam optimizer at a learning rate 0.01. We use the ‘LinkNeighborLoader’ from PyTorch Geometric to generate training mini-batches. This loader samples both positive and negative edges, along with 30 immediate neighbors and 10 secondary neighbors sampled by random walks for each node involved in

Table 1: Link prediction algorithms. “pyg” refers to PyTorch Geometric.

	Algorithm	Reference	Code	Notation
Topology based	Preferential attachment	[3]	ourselves	PA
	Common neighbors	[4]	ourselves	CN
	AdamicAdar	[5]	ourselves	AA
	Jaccard index	[4]	ourselves	JI
	Resource allocation	[6, 7]	ourselves	RA
	Local Random Walk	[8]	ourselves	LRW
	Local Path Index	[9]	ourselves	LPI
Graph embedding	Laplacian EigenMap	[10]	ourselves	EigenMap
	Spectral modularity	[11]	ourselves	Mod
	Non-backtracking embedding	[12]	ourselves	NB
	FastRP	[13]	ourselves	FastRP
	Adjacency matrix w/ the exponential kernel	[14, 15]	ourselves	Exp-A
	Laplacian w/ the exponential kernel	[14, 15]	ourselves	Exp-L
	Normalized Laplacian w/ the exponential kernel	[14, 15]	ourselves	Exp-NL
	Adjacency matrix w/ the von Neumann kernel	[15, 16]	ourselves	vN-A
	Laplacian w/ the von Neumann kernel	[15, 16]	ourselves	vN-L
	Normalized Laplacian w/ the von Neumann kernel	[15, 16]	ourselves	vN-NL
	LINE	[19]	gensim [34, 35]	LINE
DeepWalk	[18]	gensim [34, 35]	DeepWalk	
node2vec	[17]	gensim [34, 35]	node2vec	
Graph neural networks	node2vec	[17]	gensim [34, 35]	node2vec
	Graph Convolutional Network	[22]	pyg [21]	GCN
	Graph SAGE	[23]	pyg [21]	GraphSAGE
	Graph SAGE	[23]	pyg [21]	GraphSAGE
	Graph Attention Network	[24]	pyg [21]	GAT
	GIN	[25]	pyg [21]	GIN
Network model	Stochastic block model	[28–31]	graph tool [33]	SBM
	Degree-corrected stochastic block model	[31–33]	graph tool [33]	dcSBM

these edges [23]. The batch size is set to 5000.

### 1.2.4 Network models

We use two stochastic block models (SBM) [28–31] and the degree-corrected SBM [31–33]. These models estimate the probability  $P(i, j)$  that an edge exists between two nodes, which serves as the prediction score  $s_{ij}$ . We fit the SBMs using the graph tool package [33]. We select the number of blocks that minimize the description length and use default settings for other parameters.

## 1.3 Additional analysis methods

We use the following additional analysis methods in this paper. We fit a log-normal distribution to the degree distribution of the graphs by using the moment method implemented in the `scipy.stats.lognorm` package [36]. We fit a power-law distribution to the degree distribution of the graphs by using

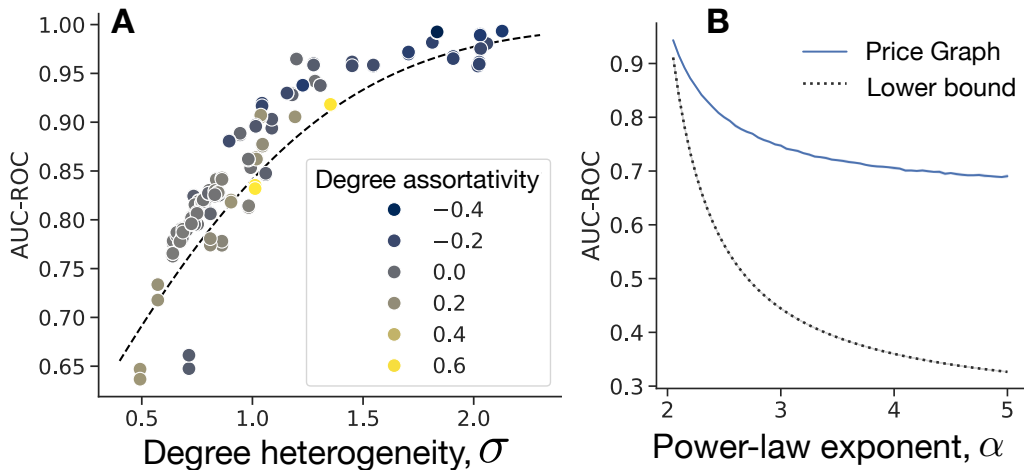


Figure 1: The AUC-ROC for PA as a function of degree heterogeneity. **A**: The AUC-ROC for the empirical graphs and that expected by node degree (Eq. (9) in the main text). The colors represent the degree assortativity. **B**: Lower bound for the AUC-ROC for the power-law degree distributions. The dashed line represents the lower bound for the AUC-ROC for the power-law distribution. The blue line represents the AUC-ROC for PA for the Price graph with  $N = 10^4$  nodes and  $M = 10^5$  edges.

the maximum likelihood method implemented in the `powerlaw` package [37]. We compute the RBO score by using the `rbo` package [38].

## 2 Robustness analysis

### 2.1 Impact of degree assortativity on the AUC-ROC for PA

We have assumed that the graph has no degree assortativity, meaning that  $P(k_i, k_j) = P(k_i)P(k_j)$ . Although this assumption may not always hold, it provides a good approximation for the AUC-ROC behavior for PA. Although the assortativity varies across graphs, the AUC-ROC for PA still closely follows Eq. (9) in the main text (Fig. 1).

## 2.2 AUC-ROC for PA for scale-free networks

We have assumed that the graph exhibits the heterogeneous degree distributions characterized by the log-normal distribution. An alternative model of the degree distribution is the power-law distribution [39]. Here, we show that our results also hold for the power-law degree distribution, i.e., the AUC-ROC for PA increases as the degree heterogeneity increases.

We compute the AUC-ROC for PA for graphs with power-law degree distribution. Computing AUC-ROC  $P(k_{i-}k_{j-} \leq k_{i+}k_{j+})$  is not trivial because it involves multiplicative convolution of two probability distributions, which are hard to compute for the power law degree distribution. To circumvent this problem, we consider the lower-bound by focusing on  $k_{i-} \leq k_{i+}$  and  $k_{j-} \leq k_{j+}$ , which is the subset of all combinations of  $(k_{i-}, k_{i+}, k_{j-}, k_{j+})$  leading to  $k_{i-}k_{j-} \leq k_{i+}k_{j+}$ , i.e.,

$$P(k_{i-} < k_{i+}) \cdot P(k_{j-} < k_{j+} \mid k_{i-}, k_{i+}) \leq P(k_{i-}k_{j-} < k_{i+}k_{j+}) \quad (1)$$

Assuming that the graph has no degree assortativity (i.e.,  $P(k_i, k_j) = P(k_i)P(k_j)$ ), we obtain the lower bound for the AUC-ROC:

$$P(k_{i-} < k_{i+}) \geq P(k_{i-} < k_{i+})^2 = \left[ \sum_{k=1}^{\infty} p_{\text{neg}}(k) \sum_{\ell=k}^{\infty} p_{\text{pos}}(\ell) \right]^2. \quad (2)$$

Now, let us compute the lower bound by assuming that the degree distribution follows a power-law [40]:

$$p(k) = \frac{1}{\zeta(\alpha, k_{\min})} k^{-\alpha}, \quad (k \geq k_{\min}), \quad \text{where } \zeta(\alpha, k_{\min}) = \sum_{\ell=k_{\min}}^{\infty} \ell^{-\alpha}, \quad (3)$$

where  $\zeta$  is the Hurwitz zeta function, and  $k_{\min}$  is the minimum degree. By substituting Eq. (1) in the main text into Eq. (3), we have  $p_{\text{pos}} = k^{-\alpha+1}/\zeta(\alpha-1, k_{\min})$ . By noting that  $\sum_{\ell=k}^{\infty} p(\ell) = \zeta(\alpha, k)/\zeta(\alpha, k_{\min})$  [40], we have

$$P(k_{i-} < k_{i+})^2 = \left[ \frac{1}{\zeta(\alpha, k_{\min})\zeta(\alpha-1, k_{\min})} \sum_{k=k_{\min}}^{\infty} k^{-\alpha} \zeta(\alpha-1, k) \right]^2. \quad (4)$$

Numerical calculation shows that the lower bound  $P(k_{i-} < k_{i+})^2$  approaches 1 as  $\alpha \rightarrow 2$  (Fig. 1). Additional validation using the Price network with

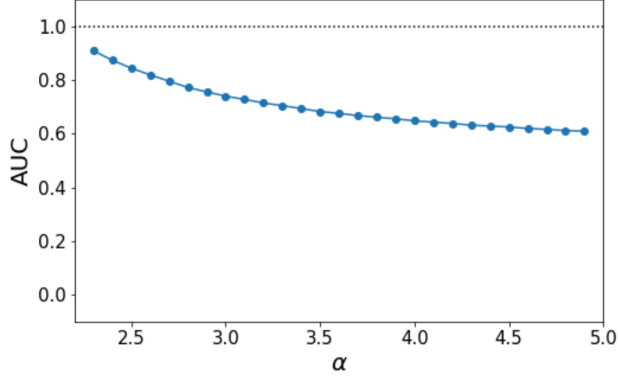


Figure 2: The influence of degree heterogeneity on the performance of the preferential attachment (PA) link prediction model in graphs with a power law degree distribution. The degree heterogeneity is governed by the power law exponent  $\alpha$ . As  $\alpha$  increases, the heterogeneity decreases. PA reaches near maximal AUC-ROC scores (1) as  $\alpha \rightarrow 2$ . For each  $\alpha$ , we generate 20 batches, each with 5000 samples of  $k_i^+, k_j^+, k_m^-, k_j^-$ . The dots indicate the average AUC score obtained via the Mann-Whitney U statistic. Standard mean errors are smaller than the dots.

$N = 10^4$  nodes and  $M = 10^5$  edges, where  $p(k) \propto k^{-\alpha}$ , confirms that PA achieves higher AUC-ROC than the lower-bound and reaches near-maximal AUC-ROC scores for  $\alpha \approx 2$ .

We can also compute the AUC score using the Mann-Whitney U statistic (Fig. 2). Let us take a graph  $G$  with the set of nodes given by  $\mathcal{V}$ . We sample nodes  $i, j$  with degrees  $k_i^+, k_j^+$  forming the positive set of edges from  $p_{pos}$ , and nodes  $m, n$  with degrees  $k_m^-, k_n^-$  forming the negative set of edges from  $p_{neg}$ . Then  $P(k_i^+ k_j^+ > k_m^-, k_n^-) \forall i, j, k, m \in \mathcal{V}$  is the AUC score and is given by  $\frac{U}{n_1 n_2}$  where  $U$  is the Mann-Whitney U statistic and  $n_1, n_2$  are sizes of the positive and negative edge sets respectively [41]. We sample the random variables  $k_i^+, k_j^+$  using the “Power\_Law” function from the powerlaw package [37] with degree exponent  $\alpha - 1$  since  $p_{pos}(k) \sim k^{-(\alpha-1)}$ . Similarly, we sample  $k_m^-, k_n^-$  with degree exponent  $\alpha$  since  $p_{neg}(k) \sim k^{-\alpha}$ . Fig. 2 aligns with our findings in Fig. 1B, i.e., PA reaches near maximal AUC-ROC scores as  $\alpha \rightarrow 2$ .

### 2.3 Parameter sensitivity in the analysis of performance alignment with the recommendation task

The vertex-centric max precision recall at  $C$  (VCMPR@C) metric [42] is a metric computed based on the precision and recall of the recommendations for each node. This metric is proposed for evaluating link prediction methods in recommendation settings. The VCMPR@C for a node  $i$  and recommended node set  $\mathcal{V}_i$  is defined as

$$\text{VCMPR@C for node } i = \frac{\sum_{j \in \mathcal{V}_i} Y_{ij}}{\max(C, m_i)}, \quad (5)$$

where  $Y_{ij}$  is the indicator function of node  $j$  is connected with  $i$  in the test data ( $Y_{ij} = 1$ ), and otherwise  $Y_{ij} = 0$ . Variable  $m_i$  is the number of true connections in the test data, i.e.,  $m_i = \sum_j Y_{ij}$ . We compute the average VCMPR@C for all nodes as the performance of the link prediction method for the graph.

We compute the similarity of two rankings with rank-biased overlap (RBO) [43]. RBO assesses the similarity of two rankings by examining the overlap of top-performing methods. Define  $U_{k,1}$  as the set of methods ranked in the top  $k$  positions in ranking 1, and  $U_{k,2}$  similarly for ranking 2. Then, RBO computes a weighted average of the similarity of the top  $k$  methods by

$$\text{RBO}(S, T, p) := (1 - p) \sum_{k=1}^{\infty} p^{k-1} \frac{|U_{k,1} \cap U_{k,2}|}{k}, \quad (6)$$

where  $p$  controls the importance of the top performer, with a smaller  $p$  value placing more weight on the top performer. We use  $p = 0.5$  for the results in the main text. We find consistent results across different  $p$  values (Fig. 3A and B). Additionally, we find consistent results for a different number of recommendations  $C$  (Fig. 3C and D).

### 2.4 Evaluation of the community detection performance using the normalized mutual information

Normalized Mutual Information (NMI) is a standard metric for assessing community detection methods [29, 44]. NMI quantifies the similarity between actual and predicted community assignments, where a score of zero indicates no similarity. We note that NMI has a bias favoring partitions with small

communities [45], and thus, we used the element-centric similarity that does not have this bias in our main experiment. We note that NMI has a bias favoring partitions with small communities [45], and thus, we used the element-centric similarity that does not have this bias in our main experiment. Nevertheless, we include the results for NMI in Fig. 4 for comparison. As with the element-centric similarity, our results show that the degree-corrected GNNs perform on par or better than the original GNNs.

## 2.5 Sensitivity to the choice of the LFR benchmark parameters

We tested the robustness of the results by using different parameter values for the LFR benchmark. First, we confirmed the consistent results when varying the average degree  $\langle k \rangle$  from 25 to 50 (Fig. 5), or the maximum community size and degree from 1000 to 500 (Fig. 6).

# 3 Reproducibility

## 3.0.1 Source data and code

The source data, code, and workflow for our experiments are available on GitHub and FigShare. The URLs are omitted in accordance with NeurIPS anonymity guidelines; however, we provide the data and code in the supplementary materials.

## 3.0.2 Snakemake workflow

We ensure the reproducibility of our experiments by using Snakemake [46], which allows automatic workflow execution from the preprocessing to the generation of the plots. With the Snakemake workflow, the user can reproduce all results by running the following command in the terminal:

```
snakemake --cores <number of cores> all
```

The workflow requires Python 3.11 or later, and all required Python packages are listed in the “environment.yaml” file in the repository.

### 3.0.3 Execution time and hardware requirements

We run the workflow on a server with 64 Intel(R) Xeon(R) Gold 5218 CPUs equipped with 64 cores, 1T RAM, and four NVIDIA GPUs with 48 GB memory, sufficient to complete the workflow in one week. The execution time of the workflow for the community detection task is 4 days, and that for the link prediction task is 10 days. The workflow can be executed with fewer resources by reducing the number of cores. The minimum computer requirements to run the workflow are as follows:

- 64 GB RAM
- 16 GB GPU memory
- 8 core CPU
- 300 GB space

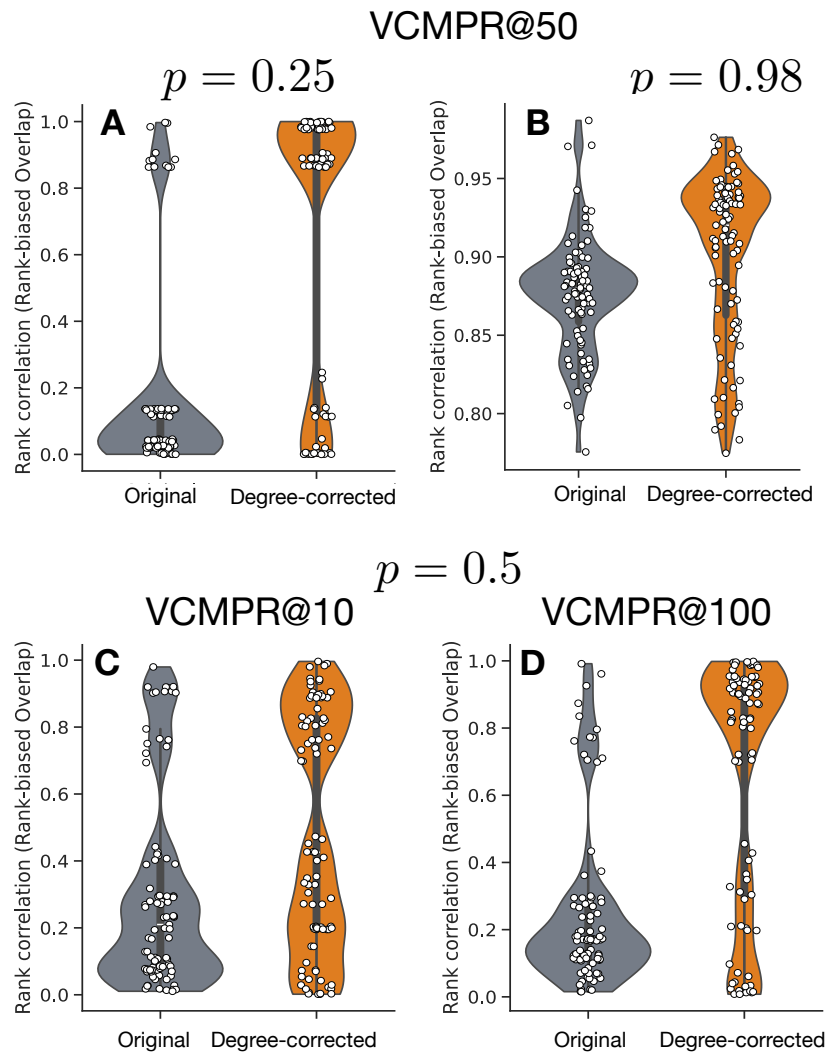


Figure 3: RBO for different  $p$  values and different numbers  $C$  of recommendations.

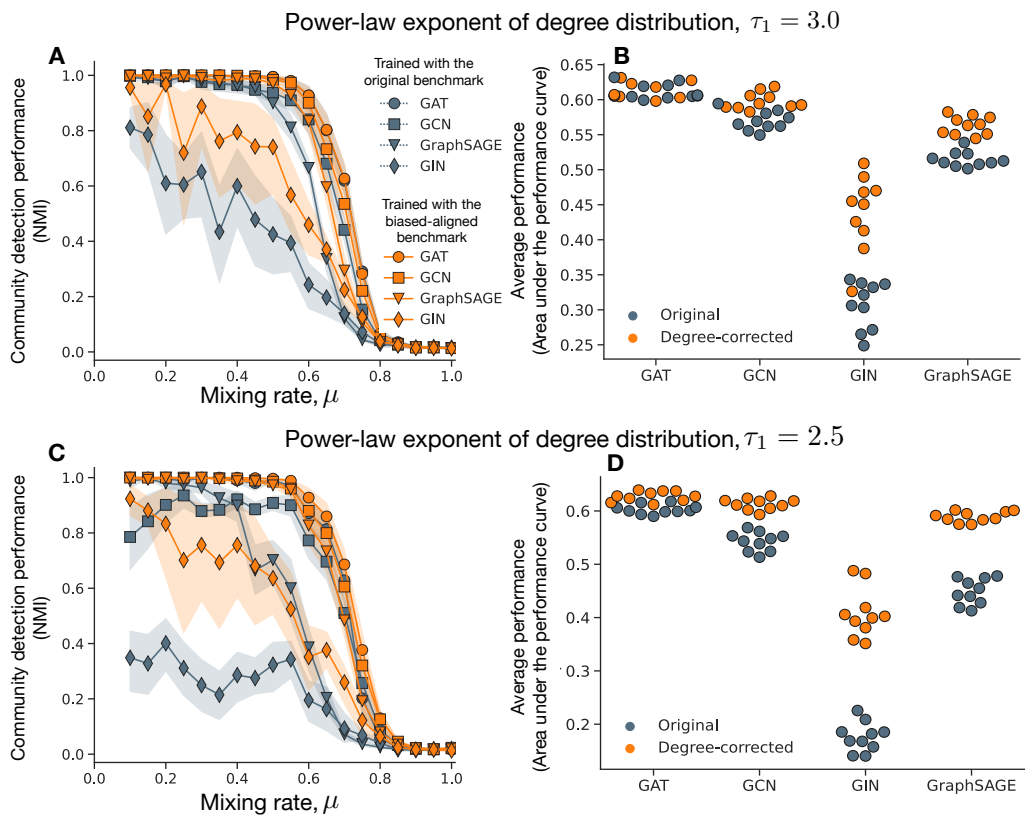


Figure 4: Performance of the GNNs on the LFR benchmark measured by NMI.

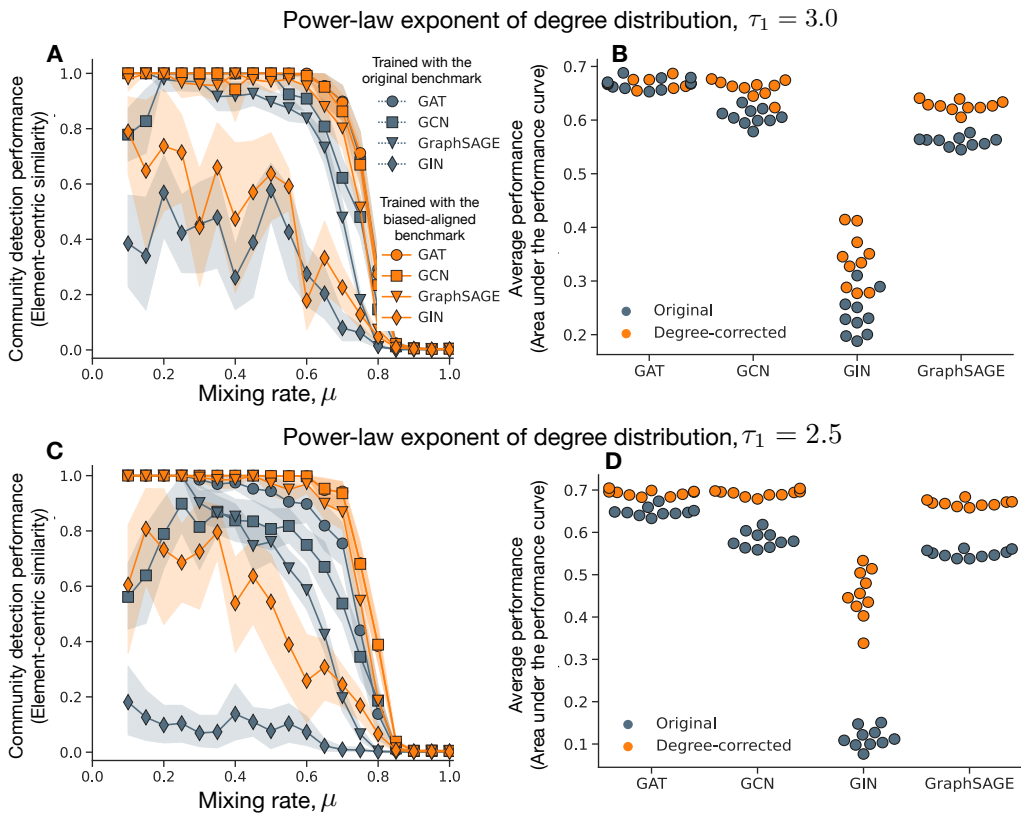


Figure 5: Performance of the GNNs on the LFR benchmark measured by NMI when varying the average degree  $\langle k \rangle$  from 25 to 50.

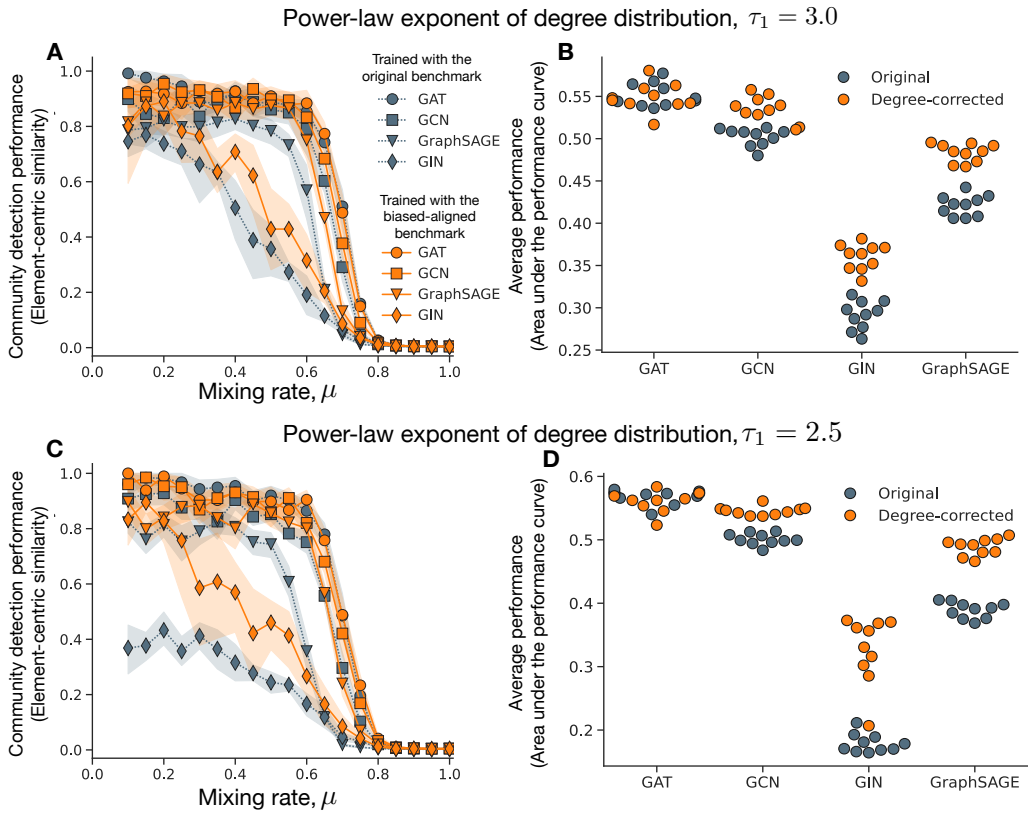


Figure 6: Performance of the GNNs on the LFR benchmark measured by NMI when varying the maximum community size and degree from 1000 to 500.

Table 2: Network data tested in this study. We consider social, technological, information, biological, and transportation (spatial) networks. For simplicity in our analysis, we consider these networks to be unweighted, undirected, and without self-loops. Variance refers to the variance of the node degrees. Assortativity refers to the degree assortativity, and Heterogeneity refers to the degree heterogeneity computed by [47].

Network	Nodes	Edges	Max. Degree	Variance	Assortativity	Heterogeneity
Political books	105	441	25	29.69	-0.128	0.43
College football	115	613	12	0.78	0.162	0.20
High school 2011	126	1709	55	153.71	0.083	0.62
Food web bay wet	128	2075	110	249.17	-0.112	0.62
Food web bay dry	128	2106	110	249.85	-0.104	0.63
Radoslaw email	167	3250	139	993.84	-0.295	0.62
Highschool 2012	180	2220	56	120.37	0.046	0.51
Little Rock Lake	183	2434	105	433.29	-0.266	0.54
Jazz	198	2742	100	303.12	0.020	0.55
C. Elegans	297	2148	134	167.56	-0.163	0.38
Network science	379	914	34	15.42	-0.082	0.23
Dublin social	410	2765	50	70.51	0.226	0.29
Airport	500	2980	145	499.03	-0.268	0.35
Caltech	762	16651	248	1365.76	-0.066	0.42
Reed	962	18812	313	1254.53	0.023	0.38
Political blogs	1222	16714	351	1474.67	-0.221	0.34
Haverford	1446	59589	375	3687.70	0.067	0.41
Simmons	1510	32984	300	1288.53	-0.062	0.32
Swarthmore	1657	61049	577	3472.20	0.061	0.37
Petster	1788	12476	272	440.86	-0.089	0.24
UC Irvine	1893	13835	255	599.57	-0.188	0.24
Yeast	2224	6609	64	63.67	-0.105	0.15
Amherst	2235	90954	467	4007.71	0.058	0.35
Bowdoin	2250	84386	670	3206.35	0.056	0.33
Hamilton	2312	96393	602	3940.69	0.031	0.34
Adolescent health	2539	10455	27	18.59	0.251	0.10
Trinity	2613	111996	404	3742.49	0.072	0.32
USFCA	2672	65244	405	2041.31	0.092	0.27
Japanese book	2698	7995	725	608.58	-0.259	0.17
Williams	2788	112985	610	3901.94	0.040	0.32
Open flights	2905	15645	242	485.44	0.049	0.21
Oberlin	2920	89912	478	2838.11	0.050	0.28
Wellesley	2970	94899	746	3079.68	0.064	0.29
Smith	2970	97133	349	2432.51	0.044	0.28
Vassar	3068	119161	482	3453.23	0.101	0.30
Middlebury	3069	124607	473	3865.24	0.078	0.30

Table 3: (Continued) Network data tested in this study.

Network	Nodes	Edges	Max. Degree	Variance	Assortativity	Heterogeneity
Pepperdine	3440	152003	674	5695.91	0.055	0.31
Colgate	3482	155043	773	4009.14	0.067	0.29
Santa	3578	151747	1129	4933.35	0.071	0.29
Wesleyan	3591	138034	549	3548.92	0.095	0.28
Mich	3745	81901	419	1997.51	0.142	0.24
Bitcoin alpha	3775	14120	511	402.89	-0.169	0.17
Bucknell	3824	158863	506	3498.69	0.094	0.27
Brandeis	3887	137561	1972	4646.98	-0.026	0.27
Howard	4047	204850	1215	8506.41	0.058	0.32
Rice	4083	184826	581	5669.22	0.065	0.29
GR-QC 1993-2003	4158	13422	81	74.41	0.639	0.12
Tennis	4338	81865	451	4573.31	0.003	0.26
Rochester	4561	161403	1224	3632.47	0.025	0.25
Lehigh	5073	198346	973	4073.33	0.035	0.24
JohnsHopkins	5157	186572	886	4761.94	0.080	0.25
HT09	5352	18481	1287	1333.44	-0.431	0.14
Wake	5366	279186	1341	7469.92	0.071	0.27
Hep-Th 1995-99	5835	13815	50	20.77	0.185	0.08
Bitcoin OTC	5875	21489	795	531.22	-0.165	0.15
Reactome	5973	145778	855	4612.48	0.241	0.21
Jung	6120	50290	5655	16029.25	-0.233	0.16
Gnutella Aug 08 2002	6299	20776	97	72.95	0.036	0.11
American	6370	217654	930	3847.11	0.066	0.22
MIT	6402	251230	708	6241.81	0.120	0.24
JDK	6434	53658	5923	16112.86	-0.223	0.16
William	6472	266378	1124	5164.22	0.052	0.23
U Chicago	6561	208088	1624	4093.91	0.018	0.22
Princeton	6575	293307	628	6164.10	0.091	0.24
Carnegie	6621	249959	840	5674.47	0.122	0.24
Tufts	6672	249722	827	4525.50	0.118	0.22
UC	6810	155320	660	2297.32	0.125	0.19
Wikipedia elections	7066	100736	1065	3332.59	-0.083	0.21
English book	7377	44205	2568	3699.80	-0.237	0.16
Gnutella Aug 09 2002	8104	26008	102	66.74	0.033	0.09

Table 4: (Continued) Network data tested in this study.

Network	Nodes	Edges	Max. Degree	Variance	Assortativity	Heterogeneity
French book	8308	23832	1891	1217.86	-0.233	0.12
Hep-Th 1993-2003	8638	24806	65	41.61	0.239	0.08
Gnutella Aug 06 2002	8717	31525	115	51.87	0.052	0.09
Gnutella Aug 05 2002	8842	31837	88	54.66	0.015	0.09
PGP	10680	24316	205	65.24	0.238	0.09
Gnutella Aug 04 2002	10876	39994	103	48.65	-0.013	0.08
Hep-Ph 1993-2003	11204	117619	491	2307.04	0.630	0.16
Spanish book 1	11558	43050	2986	3353.23	-0.282	0.12
DBLP citations	12495	49563	709	284.34	-0.046	0.10
Spanish book 2	12643	55019	5169	6953.72	-0.290	0.11
Cond-Mat 1995-99	13861	44619	107	45.70	0.157	0.07
Astrophysics 1	14845	119652	360	472.92	0.228	0.11
Astrophysics 2	17903	196972	504	961.58	0.201	0.11
Cond-Mat 1993-2003	21363	91286	279	119.00	0.125	0.07
Gnutella Aug 25 2002	22663	54693	66	28.58	-0.173	0.04
Internet	22963	48436	2390	1085.20	-0.198	0.08
Thesaurus	23132	297094	1062	1993.31	-0.048	0.12
Cora	23166	89157	377	123.05	-0.055	0.07
AS Caida	26475	53381	2628	1113.83	-0.195	0.08
Gnutella Aug 24 2002	26498	65359	355	35.03	-0.008	0.04

## References

- [1] Tiago P Peixoto. “The Netzschleuder network catalogue and repository”. In: URL <https://networks.skewed.de> (2020).
- [2] Şirag Erkol, Claudio Castellano, and Filippo Radicchi. “Systematic comparison between methods for the detection of influential spreaders in complex networks”. In: *Scientific Reports* 9.1 (2019), p. 15095.
- [3] Albert-László Barabási and Márton Pósfai. *Network Science*. 1st edition. Cambridge, United Kingdom: Cambridge University Press, 2016. ISBN: 978-1-107-07626-6.
- [4] David Liben-Nowell and Jon Kleinberg. “The Link Prediction Problem for Social Networks”. In: *Proceedings of the Twelfth International Conference on Information and Knowledge Management*. CIKM '03. New Orleans, LA, USA: Association for Computing Machinery, 2003, pp. 556–559. ISBN: 1581137230. DOI: [10.1145/956863.956972](https://doi.org/10.1145/956863.956972). URL: <https://doi.org/10.1145/956863.956972>.
- [5] Lada A Adamic and Eytan Adar. “Friends and neighbors on the web”. In: *Social Networks* 25.3 (2003), pp. 211–230.
- [6] Tao Zhou et al. “Bipartite network projection and personal recommendation”. In: *Physical Review E* 76.4 (2007), p. 046115.
- [7] Tao Zhou, Linyuan Lü, and Yi-Cheng Zhang. “Predicting missing links via local information”. In: *The European Physical Journal B* 71 (2009), pp. 623–630.
- [8] Weiping Liu and Linyuan Lü. “Link prediction based on local random walk”. In: *Europhysics Letters* 89.5 (2010), p. 58007.
- [9] Linyuan Lü, Ci-Hang Jin, and Tao Zhou. “Similarity index based on local paths for link prediction of complex networks”. In: *Phys. Rev. E* 80 (4 Oct. 2009), p. 046122. DOI: [10.1103/PhysRevE.80.046122](https://link.aps.org/doi/10.1103/PhysRevE.80.046122). URL: <https://link.aps.org/doi/10.1103/PhysRevE.80.046122>.
- [10] Mikhail Belkin and Partha Niyogi. “Laplacian Eigenmaps for Dimensionality Reduction and Data Representation”. In: *Neural Computation* 15.6 (2003), pp. 1373–1396. ISSN: 0899-7667.
- [11] Raj Rao Nadakuditi and M. E. J. Newman. “Graph Spectra and the Detectability of Community Structure in Networks”. In: *Physical Review Letters* 108.18 (2012), p. 188701.

- [12] Florent Krzakala et al. “Spectral Redemption in Clustering Sparse Networks”. In: *Proceedings of the National Academy of Sciences* 110.52 (2013), pp. 20935–20940.
- [13] Haochen Chen et al. “Fast and accurate network embeddings via very sparse random projection”. In: *Proceedings of the 28th ACM International Conference on information and knowledge management*. 2019, pp. 399–408.
- [14] Risi Imre Kondor and John Lafferty. “Diffusion kernels on graphs and other discrete structures”. In: *Proceedings of the 19th International Conference on Machine Learning*. Vol. 2002. 2002, pp. 315–322.
- [15] Jérôme Kunegis and Andreas Lommatzsch. “Learning spectral graph transformations for link prediction”. In: *Proceedings of the 26th Annual International Conference on Machine Learning*. 2009, pp. 561–568.
- [16] Takahiko Ito et al. “Application of kernels to link analysis”. In: *Proceedings of the eleventh ACM SIGKDD International Conference on Knowledge discovery in data mining*. 2005, pp. 586–592.
- [17] Aditya Grover and Jure Leskovec. “Node2vec: Scalable Feature Learning for Networks”. In: *Proceedings of the 22nd ACM SIGKDD International Conference on KDD*. KDD ’16. New York, NY, USA: Association for Computing Machinery, 2016, pp. 855–864. ISBN: 978-1-4503-4232-2.
- [18] Bryan Perozzi, Rami Al-Rfou, and Steven Skiena. “DeepWalk: Online Learning of Social Representations”. In: *Proceedings of the 20th ACM SIGKDD International Conference on KDD*. KDD ’14. New York, NY, USA: Association for Computing Machinery, 2014, pp. 701–710. ISBN: 978-1-4503-2956-9.
- [19] Jian Tang et al. “LINE: Large-scale Information Network Embedding”. In: *Proceedings of the 24th International Conference on World Wide Web*. WWW ’15. Republic and Canton of Geneva, CHE: International World Wide Web Conferences Steering Committee, 2015, pp. 1067–1077. ISBN: 978-1-4503-3469-3.
- [20] Sadamori Kojaku et al. “Network community detection via neural embeddings”. In: *arXiv preprint arXiv:2306.13400* (2023).
- [21] Matthias Fey and Jan Eric Lenssen. “Fast graph representation learning with PyTorch Geometric”. In: *arXiv preprint arXiv:1903.02428* (2019).

- [22] Thomas N. Kipf and Max Welling. “Semi-Supervised Classification with Graph Convolutional Networks”. In: *International Conference on Learning Representations (ICLR)*. 2017.
- [23] Will Hamilton, Zhitao Ying, and Jure Leskovec. “Inductive representation learning on large graphs”. In: *Advances in Neural Information Processing Systems* 30 (2017).
- [24] Petar Veličković et al. “Graph Attention Networks”. In: *International Conference on Learning Representations* (2018). accepted as poster. URL: <https://openreview.net/forum?id=rJXMpikCZ>.
- [25] Keyulu Xu et al. “How powerful are graph neural networks?” In: *arXiv preprint arXiv:1810.00826* (2018).
- [26] Ryoma Sato, Makoto Yamada, and Hisashi Kashima. “Random features strengthen graph neural networks”. In: *Proceedings of the 2021 SIAM International Conference on data mining (SDM)*. SIAM. 2021, pp. 333–341.
- [27] Ralph Abboud et al. “The Surprising Power of Graph Neural Networks with Random Node Initialization”. In: *International Joint Conference on Artificial Intelligence*. 2020. URL: <https://api.semanticscholar.org/CorpusID:222134198>.
- [28] Santo Fortunato. “Community Detection in Graphs”. In: *Physics Reports* 486.3 (2010), pp. 75–174. ISSN: 0370-1573.
- [29] Santo Fortunato and Darko Hric. “Community Detection in Networks: A User Guide”. In: *Physics Reports. Community Detection in Networks: A User Guide* 659 (2016), pp. 1–44. ISSN: 0370-1573.
- [30] Santo Fortunato and Mark E. J. Newman. “20 Years of Network Community Detection”. In: *Nature Physics* 18.8 (2022), pp. 848–850. ISSN: 1745-2481.
- [31] Tiago P. Peixoto. “Parsimonious Module Inference in Large Networks”. In: *Physical Review Letters* 110.14 (2013), p. 148701.
- [32] Brian Karrer and M. E. J. Newman. “Stochastic Blockmodels and Community Structure in Networks”. In: *Physical Review E* 83.1 (2011), p. 016107.
- [33] *Graph-Tool: Efficient Network Analysis with Python*. <https://graph-tool.skewed.de/>.

- [34] Radim Rehurek and Petr Sojka. “Gensim–python framework for vector space modelling”. In: *NLP Centre, Masaryk University, Czech Republic* 3.2 (2011).
- [35] Louis Abraham. *fastnode2vec*. 2020. DOI: [10.5281/zenodo.3902632](https://doi.org/10.5281/zenodo.3902632). URL: <https://github.com/louisabraham/fastnode2vec>.
- [36] Pauli Virtanen et al. “SciPy 1.0: Fundamental Algorithms for Scientific Computing in Python”. In: *Nature Methods* 17 (2020), pp. 261–272.
- [37] Jeff Alstott, Ed Bullmore, and Dietmar Plenz. “powerlaw: a Python package for analysis of heavy-tailed distributions”. In: *PloS ONE* 9.1 (2014), e85777.
- [38] *GitHub changyaochen/rbo*. <https://github.com/changyaochen/rbo>. [Accessed 26-Apr-2024].
- [39] Albert-László Barabási and Eric Bonabeau. “Scale-free networks”. In: *Scientific american* 288.5 (2003), pp. 60–69.
- [40] Aaron Clauset, Cosma Rohilla Shalizi, and Mark EJ Newman. “Power-law distributions in empirical data”. In: *SIAM review* 51.4 (2009), pp. 661–703.
- [41] Simon J Mason and Nicholas E Graham. “Areas beneath the relative operating characteristics (ROC) and relative operating levels (ROL) curves: Statistical significance and interpretation”. In: *Quarterly Journal of the Royal Meteorological Society: A Journal of the Atmospheric Sciences, Applied Meteorology and Physical Oceanography* 128.584 (2002), pp. 2145–2166.
- [42] Nicolas Menand and C Seshadhri. “Link prediction using low-dimensional node embeddings: The measurement problem”. In: *Proceedings of the National Academy of Sciences* 121.8 (2024), e2312527121.
- [43] William Webber, Alistair Moffat, and Justin Zobel. “A Similarity Measure for Indefinite Rankings”. In: *ACM Trans. Inf. Syst.* 28.4 (Nov. 2010). ISSN: 1046-8188. DOI: [10.1145/1852102.1852106](https://doi.org/10.1145/1852102.1852106). URL: <https://doi.org/10.1145/1852102.1852106>.
- [44] Andrea Lancichinetti and Santo Fortunato. “Community detection algorithms: a comparative analysis”. In: *Physical Review E* 80.5 (2009), p. 056117.

- [45] Alexander J. Gates et al. “Element-Centric Clustering Comparison Unifies Overlaps and Hierarchy”. In: *Scientific Reports* 9.1 (2019), p. 8574. ISSN: 2045-2322.
- [46] Johannes Köster and Sven Rahmann. “Snakemake—a scalable bioinformatics workflow engine”. In: *Bioinformatics* 28.19 (2012), pp. 2520–2522.
- [47] Rinku Jacob et al. “Measure for degree heterogeneity in complex networks and its application to recurrence network analysis”. In: *Royal Society open science* 4.1 (2017), p. 160757.